

# Impact Analysis of Land Use on Time Lag and Peak Discharge in the Downstream Area of Sadia Watershed Bima City West Nusa Tenggara using HEC-HMS and SCS-CN

I Putu Hartawan<sup>1\*</sup>, Firmana Siddik<sup>1</sup>, Ary Firmana<sup>1</sup>, Ekanto Wahyudi Susetyo<sup>1</sup>, Dhemi Harlan<sup>1</sup>, Bagus Handyastono<sup>2</sup>, Mohammed AS Algoul<sup>3</sup>

<sup>1</sup> Water Resources Management, Faculty of Civil and Environmental Engineering, Bandung Institute of Technology  
Jl. Ganesa No. 10. Coblong, Bandung City, West Java, Indonesia 40132

<sup>2</sup> PT. INAKKO Internasional Konsulindo, Jl. Kramat Sentiong No. 46, Kramat, Senen, Central Jakarta City,  
Jakarta Indonesia 10450,

<sup>3</sup> Ain Al-Qarar Company, Al-Ni'mah Tower, Al-Rimal District, Gaza City, Gaza Strip, Palestine P900

Submitted: May 25<sup>th</sup>, 2025; Revised: July 18<sup>th</sup>, 2025; Accepted: July 21<sup>st</sup>, 2025; Available online: July 22<sup>nd</sup>, 2025  
DOI: 10.14710/teknik.v46i3.75074

## Abstract

Flood events have frequently occurred in the downstream area of the Sadia Watershed (DAS) in Bima City, West Nusa Tenggara. In recent years, the overflow of the Sadia River has been triggered by land use changes and the impacts of climate change. This study aims to analyze land cover changes in 2015, 2019, and 2022, and to evaluate their impact on flood peak discharge using hydrological simulations. Land cover data were analyzed using ArcMap software and integrated with hydrological modeling using HEC-HMS. The Synthetic Unit Hydrograph (HSS) SCS-CN method was used in the simulation with a 25-year return period, following calibration of the Sadia River's bank full discharge to ensure model accuracy. The simulation results showed an increase in the peak discharge entering the Sadia River, from 156,20 m<sup>3</sup>/s in 2015 to 164,80 m<sup>3</sup>/s in 2019, and 167,00 m<sup>3</sup>/s in 2022. Additionally, the time lag decreased from 445.15 minutes in 2015 to 431.84 minutes in 2019 and 429.88 minutes in 2022. The increase in the Curve Number (CN) value and impermeable area indicates a reduction in soil infiltration capacity due to land conversion. However, climate factors, such as increased rainfall intensity, also contributed to the rise in peak discharge. These findings can serve as a basis for better land use management and emphasize the importance of considering climate factors when designing flood risk mitigation efforts, especially in the face of increasing flood events.

**Keywords:** land use change; peak discharge; time lag; HEC-HMS modeling; SCS-CN

## 1. Introduction

Indonesia is a country of many islands with high rainfall and complex geography. A combination of natural factors and human activities makes Indonesia highly vulnerable to flooding, particularly during the rainy season. Various regions in Indonesia experience flooding annually, on both small and large scales, resulting in significant social, economic, and environmental losses (Farid et al. 2020; Formánek et al. 2013; Gunawan et al. 2016; Juliana et al. 2017; Kardhana et al. 2022; Kuntoro et al. 2017a; Rizaldi, Syahril, et al. 2022). Flood events in Bima City occur almost annually and are classified as significant hydrometeorological disasters, with the potential to cause damage to infrastructure, residential areas, and disrupt socio-economic activities. One of the primary

causes of these floods is the overflow of the Sadia River, which is unable to accommodate the flood discharge from the upstream area of the Sadia Watershed, resulting in the inundation of surrounding areas. The Sadia River itself is situated in the downstream section of the Sadia Watershed. In general, the contributing factors to flooding in this region include high rainfall intensity, the basin-shaped topography of Bima City, the loss of river buffer zones due to their conversion into residential areas, sedimentation in the downstream river channel, inadequate urban drainage systems, and a decline in upstream vegetative cover (Yuniartanti, 2018). The upstream area of the Sadia Watershed covers parts of Bima Regency and Bima City, consisting of various land use classifications, including protected forest, production forest, conservation forest, and Other Land Use Areas (APL) (Adi and Muladi, 2022). Based on data from the Ministry of Environment and Forestry (KLHK), the area of critical land in Bima City covers

\*) Corresponding Author.  
E-mail: [iputuhartawan84@gmail.com](mailto:iputuhartawan84@gmail.com)

3,935.92 ha, slightly critical land covers 2,707.80 ha, potentially critical land covers 12,933.63 ha, and non-critical land covers 1,576.97 ha (Yuniartanti, 2018). The extensive area of critical land indicates a high level of environmental degradation, which can lead to an increase in peak discharge and a reduction in soil infiltration capacity (Kuntoro et al. 2017b). The expansion of agricultural activities, particularly for high-economic-value corn commodities, has driven massive land conversion, including areas of forest that should be protected. This land use change has increased the extent of impervious surfaces, contributing to higher surface runoff and raising the potential for pluvial flooding in downstream areas (Yosua, Kusuma, and Nugroho 2023). Changes in watershed characteristics, such as increased maximum rainfall intensity and reduced vegetative cover, have been proven to affect the rise in flood discharge (Mufrodi and Sriyana 2024).

Previous studies related to the climate classification of Sumbawa Island, where Bima City is located, have shown fluctuations in the values of the Precipitation Effectiveness (PE) and Thermal Efficiency (TE) indices, indicating shifts in regional climate patterns. The PE index, which represents the ratio of effective precipitation to evaporation, is used to assess climatic water availability, while the TE index (thermal efficiency index) measures the influence of temperature on climate formation (Ariffin, 2019). Furthermore, the Q value (the ratio of wet months to dry months), calculated using the Schmidt-Fergusson method, indicates a shift in climate classification. Regions previously categorized under dry and semi-dry climate types (E and F) have experienced a transition from a more balanced climate condition toward increasingly drier conditions, intensifying the impacts of drought and rainfall pattern variability across Sumbawa Island, including in Bima City (Yasa et al. 2023).

To date, no quantitative study has comprehensively analyzed the impact of land cover changes on peak discharge and time lag entering the Sadia River. Therefore, this study aims to analyze land cover changes in 2015, 2019, and 2022, and to evaluate their impact on flood peak discharge using hydrological simulations with HEC-HMS 4.12. The analysis employs a Synthetic Unit Hydrograph (SUH) approach, specifically the SCS Unit Hydrograph method.

## 2. Materials and Methods

The rainfall data used in this study were obtained from the Global Precipitation Measurement (GPM) satellite and are openly accessible via the official NASA Giovanni data portal (<https://giovanni.gsfc.nasa.gov/giovanni/>). This dataset has been widely validated in hydrological studies, particularly in regions with limited ground-based observation data. According to the Rainfall Analysis Module (Balai Teknik Bendungan 2022), satellite

precipitation data can be utilized when observational data are spatially and temporally limited.

Rainfall data for the hydrological analysis in this study were obtained from the GPM satellite, covering a 24-year period (2001–2024). The GPM data were calibrated using observational data from the Kumbe Rainfall Observation Station (PCH), provided by Basin Organization for Nusa Tenggara I River (BBWS NT I) Mataram. Topographic data were acquired from the National Digital Elevation Model (DEMNAS), while land cover data for the years 2015, 2019, and 2022 were sourced from the Ministry of Environment and Forestry (KLHK). Soil type data were obtained from the Global Hydrologic Soil Group. All these datasets were utilized for watershed parameterization in the hydrological modeling process using the HEC-HMS software. Flood discharge estimation was carried out using the Synthetic Unit Hydrograph (SUH) approach, specifically employing the SCS Unit Hydrograph (SCS-UH) method.

HEC-HMS is hydrological modeling software that simulates surface runoff in watersheds using the rainfall-runoff approach. It accounts for components such as infiltration, evapotranspiration, baseflow, and routing, making it suitable for flood analysis and water resource planning. The SCS-CN method estimates surface runoff based on soil type, land use, and initial moisture conditions. The CN value simplifies runoff estimation and is widely used in hydrological studies. The calculated flood discharge was then calibrated against the river's bankfull discharge (with a 2-year return period), based on river cross-section geometry data from 2022 obtained from the BBWS NT I Mataram.

### 2.1 Land Use Change Analysis

In general, land cover refers to the physical characteristics of the Earth's surface that can be directly observed, such as forests, rice fields, and settlements. In contrast, land use describes the functional and purposeful utilization of land by humans, including residential areas, agriculture, and industrial zones. Land cover data were processed using ArcGis Pro version 3.5 to produce land cover maps for each respective year. Through spatial overlay and temporal analysis, land cover changes over time were identified, including trends in land conversion such as the transformation of forest areas into settlements or other built-up areas. Changes in land use, which frequently take place in certain regions, are also a significant factor contributing to flooding and should be taken into account (Handyastono et al. 2025). The resulting land cover map was then used as input parameters in hydrological modeling using HEC-HMS software, namely the parameters Initial Abstraction ( $I_a$ ), Curve Number (CN) dan Impervious (Imp). The objective of this process is to assess the impact of land use changes on the hydrological characteristics of the watershed, particularly in influencing the CN values, which directly affect surface runoff and flood potential. Land

cover plays a significant role in determining peak discharge, where an increase in impervious area leads to higher runoff volumes and greater peak discharge rates (Sachro et al. 2017). Therefore, it is essential to select a method that is appropriate to the watershed's characteristics (Sultan et al. 2022). This study is still limited to a spatial-technical approach, focusing solely on analyzing how land cover changes (such as agriculture, settlements, and others) are distributed within the Sadia Watershed and their impact on flood discharge in the downstream area. It does not include field verification or an in-depth review of spatial planning policies.

**2.2 Hydrological Analysis**

The hydrological analysis was conducted through rainfall calculations using satellite precipitation data from Global Precipitation Measurement (GPM) spanning 24 years (2001-2024), which were calibrated and correlation-tested against rainfall data from Rainfall Observation Station (PCH). This was followed by rainfall return period analysis for intervals of 2, 5, 10, 25, 50, and 100 years. The design rainfall was distributed using the PSA 007 distribution over a 6-hour period. Utilization of GPM satellite rainfall data in HEC-HMS simulations demonstrated accurate flood discharge estimation following calibration (Hartyan 2024). Subsequently, land cover analysis was conducted to determine Curve Number (CN) values for each period, which were then used to compute the design flood discharge.

The Curve Number (CN) is a dimensionless parameter representing watershed characteristics, including soil type, vegetative cover, land use, antecedent moisture conditions, and soil conservation practices (Triatmodjo 2019). CN values range from 0 to 100, where higher values indicate increased surface impermeability. CN determination requires comprehensive analysis of land cover within the study watershed. The CN value is calculated using Equation (1).

$$CN = \left( \frac{\sum A_i CN_i}{A_i} \right) \tag{1}$$

where  $A_i$  is area of land cover type and  $CN_i$  is Curve Number value for land cover type.

The initial abstraction ( $I_a$ ) is calculated using Equation (2), with the potential maximum retention given in Equation (3).

$$I_a : 0.2 S \tag{2}$$

$$S = \frac{25400}{CN} - 254 \tag{3}$$

where  $I_a$  is Initial abstraction in (mm) and  $S$  is Potential maximum retention in (mm).

**2.3 Design Flood Discharge Analysis**

The Sadia Watershed, located in Bima City, serves as the capital area of the regency/municipality. Therefore, in the design flood discharge analysis, the

river is required to accommodate a design discharge with a return period ranging from  $Q_{10}$  to  $Q_{20}$  (PUPR 2021). However, in this study, a flood discharge with a  $Q_{25}$  return period was applied to obtain a more conservative estimate for flood management planning. Subsequently, the hydrological parameters such as Curve Number (CN), Time Lag ( $T_1$ ), and Initial Abstraction ( $I_a$ ) were utilized to calculate the effective rainfall. Effective rainfall is defined as the portion of total rainfall that directly contributes to surface runoff. This calculation was performed through hydrological modeling using the HEC-HMS software (Taufik et al. 2022) (Merwade 2022). To convert effective rainfall into design flood discharge, a Synthetic Unit Hydrograph (SUH) approach was applied using the SCS Unit Hydrograph method, with simulations conducted for a 25-year return period to obtain the peak flood discharge. Furthermore, a comparison was made between the 2-year return period design discharge ( $Q_2$ ) and the observed bankfull discharge in the field, specifically at the section of the Sadia River that remains unaffected by river engineering interventions.

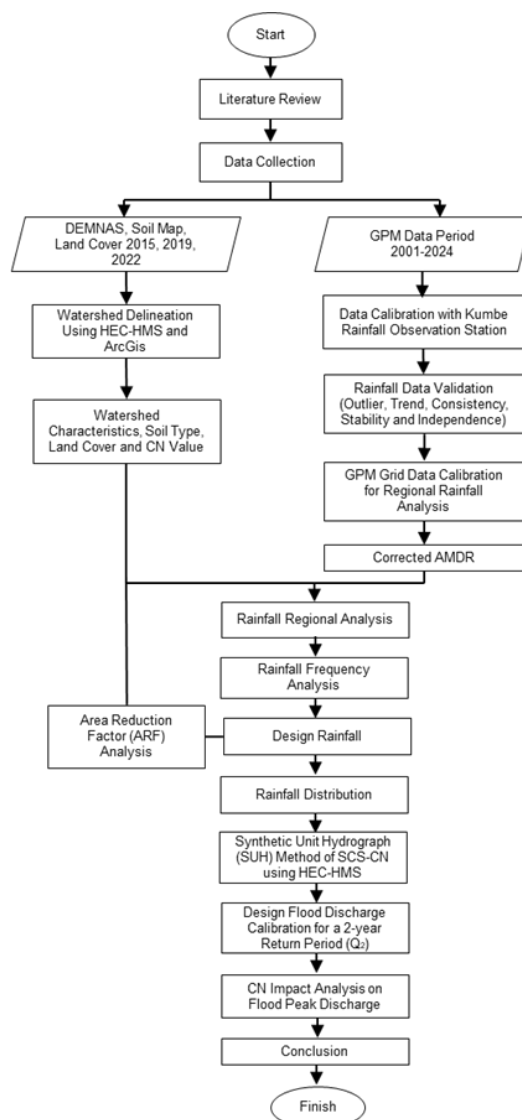


Figure 1. Research Flow Diagram.

3. Results and Discussion

3.1 Sadia Watershed Delineation

The delineation of the Sadia Watershed was conducted using HEC-HMS version 4.12 by specifying a control point (break point) located at the downstream end of the watershed as the outlet. Based on the delineation results, the total watershed area was determined to be 69.64 km<sup>2</sup>, which was further divided into 11 sub-watersheds labeled S-1 to S-11. Table 1 presents the detailed characteristics of each sub-watershed. Additionally, the watershed boundary mapping was visualized using ArcGis Pro version 3.5 and is illustrated in Figure 2. The delineation results served as the basis for spatial analysis and for integrating hydrological and land use data within the hydrological modeling framework (Merwade 2022).

Table 1. Sadia Watershed Delineation Results.

No	Sub-Watershed	Area (A) (km <sup>2</sup> )	Main Channel Length (L) (km)	Main Channel Slope (S) (m/m)	Basin Slope (m/m)
1	S-1	6.08	6.29	0.14	0.50
2	S-2	3.93	5.60	0.14	0.47
3	S-3	9.58	8.26	0.06	0.24
4	S-4	3.21	5.33	0.13	0.46
5	S-5	8.63	9.23	0.05	0.37
6	S-6	12.75	10.92	0.11	0.48
7	S-7	12.32	11.51	0.04	0.36
8	S-8	10.66	11.80	0.04	0.33
9	S-9	0.21	1.13	0.07	0.50
10	S-10	1.30	3.55	0.04	0.10
11	S-11	0.97	1.82	0.004	0.04
Jumlah		69.64	75.43		

Table 2. Summary of Land Use Area (2015–2022).

Land Use	Yr. 2015		Yr. 2019		Yr. 2022	
	Area (Km <sup>2</sup> )	%	Area (Km <sup>2</sup> )	%	Area (Km <sup>2</sup> )	%
Secondary dryland forest	22.07	31.69	33.10	47.54	24.25	34.82
Planted forest	0.00	0.00	0.00	0.00	6.51	9.35
Residential	2.12	3.04	2.22	3.19	2.35	3.37
Dryland agriculture	8.83	12.67	13.48	19.35	26.05	37.41
Dryland agriculture mixed with shrubs	17.87	25.67	14.17	20.35	0.66	0.94
Savanna	0.00	0.00	0.10	0.14	0.21	0.31
Rice field	6.24	8.97	6.20	8.91	5.86	8.41
Shrubland/ bushland	12.51	17.96	0.27	0.39	3.75	5.39
Bare Ground	0.00	0.00	0.09	0.13	0.00	0.00
<b>Total</b>	<b>69.63</b>	<b>100.00</b>	<b>69.63</b>	<b>100.00</b>	<b>69.63</b>	<b>100.00</b>

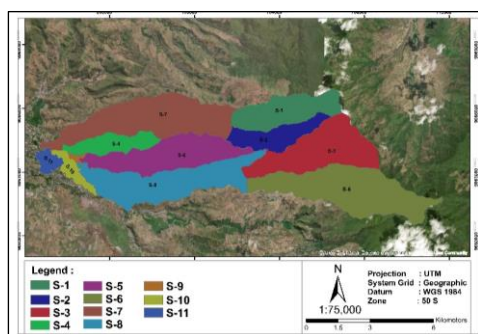


Figure 2. Sadia Watershed Delineation Map.

3.2 Topography and Soil Type Conditions

Based on the topographic analysis using ArcGis Pro version 3.5 and referring to the slope classification according to the Regulation of the Ministry of Environment and Forestry Number 10 of 2022, the topography of the Sadia Watershed is predominantly characterized by steep (25–40%) to very steep (>45%) slope classes. Areas with slopes of 25–40% and >45% (marked in brown and red on the map) are widely distributed in the middle to upstream parts of the watershed. Meanwhile, areas with gentle slopes (0–8%) are limited to the downstream section of the watershed. The topographic map of the Sadia Watershed is presented in Figure 3. In addition, the soil type analysis of the Sadia Watershed identifies two soil texture and Hydrologic Soil Group (HSG) classifications: Clay Loam with HSG D, and Sandy Clay Loam with HSG C, as shown in Figure 4.

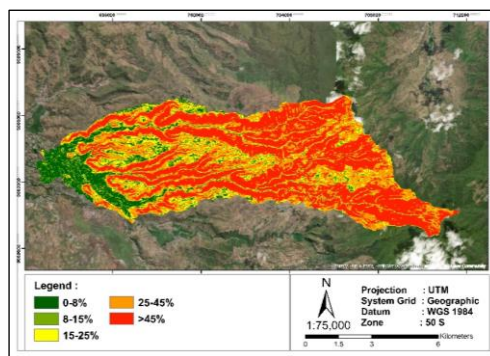


Figure 3. Sadia Watershed Topography Map.

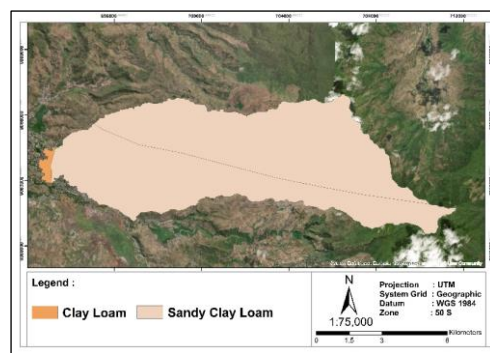


Figure 4. Soil Type Map Sadia Watershed.

3.3 Overview of Land Use Change in the Sadia Watershed

Land use in the Sadia Watershed in 2015, 2019, and 2022 was predominantly characterized by secondary dryland forest and dryland agriculture. In 2015, secondary dryland forest mixed with shrubs covered the largest area. By 2019, secondary dryland forest and mixed shrubs remained dominant; however, dryland agriculture experienced a significant increase. In 2022, land use was still dominated by secondary dryland forest, with dryland agricultural areas continuing to expand substantially. The total land use area within the Sadia Watershed remained constant at 69.64 km<sup>2</sup> throughout the three observation years. Simultaneous changes in land cover and increases in

maximum rainfall intensity have led to higher Curve Number (CN) values and surface runoff discharge, particularly in urban and industrial areas (Rizaldi, Kusuma, et al. 2022). Based on the analysis results, land use in the Sadia Watershed exhibited dynamic changes in 2015, 2019, and 2022, as illustrated in Figure 6. The area of secondary dryland forest increased significantly from 31.69% (22.07 km<sup>2</sup>) in 2015 to 47.54% (33.10 km<sup>2</sup>) in 2019, then decreased to 34.82% (24.25 km<sup>2</sup>) in 2022, although this figure remained higher than in 2015. Residential areas showed a gradual increase from 3.04% (2.12 km<sup>2</sup>) in 2015 to 3.19% (2.22 km<sup>2</sup>) in 2019 and 3.37% (2.35 km<sup>2</sup>) in 2022. The most dominant land use type was dryland agriculture, which consistently increased from 12.67% (8.83 km<sup>2</sup>) in 2015 to 19.35% (13.48 km<sup>2</sup>) in 2019 and reached 37.41% (26.05 km<sup>2</sup>) in 2022. Other changes included a reduction in the area of dryland agriculture mixed with shrubs, as well as a significant decrease in shrubland/bushland areas. The complete land use data are presented in Table 2, while the land use change maps are shown in Figure 6.

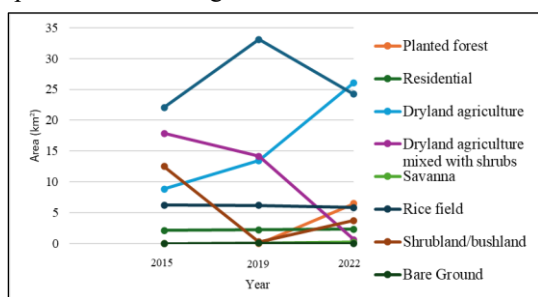
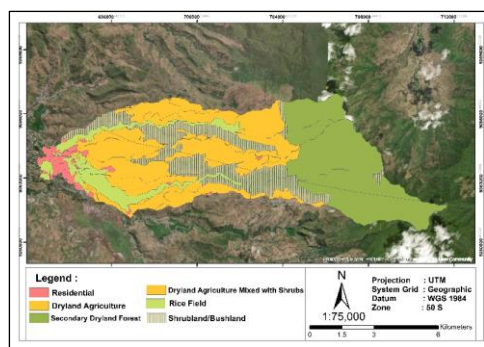
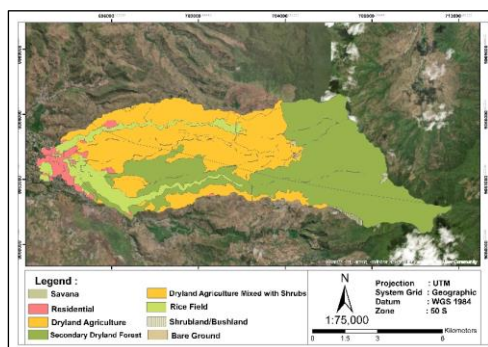


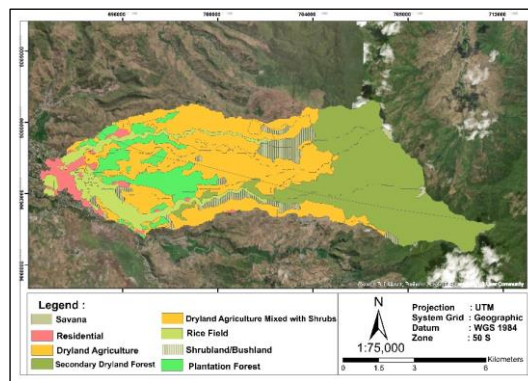
Figure 5. Land Use Change Graph in Sadia Watershed.



(a)



(b)



(c)

Figure 6. Land Use Map of Sadia Watershed in (a) 2015, (b) 2019, and (c) 2022.

Based on the Spatial Planning Map (RTRW) of Bima City for the period 2011–2031, most of the area is categorized under the planned land use of "other uses". However, land use data from 2015 and 2022 show that the majority of this area has been utilized for dryland farming. This condition highlights the need for further clarification and specification of the "other uses" category in order to assess whether the current land utilization aligns with the intended spatial designation, or whether adjustments through more specific spatial policy interventions are required.

### 3.4 Hydrological Analysis

#### 3.4.1 Calibration and Correlation Test of Satellite Rainfall Data

The rainfall data used in this test consisted of annual maximum daily rainfall data from the Kumbe Rainfall Observation Station (PCH) for the period 2011–2024. The data testing procedures included outlier test, trend test, stability test, and independence test. The results showed that the rainfall data from Kumbe PCH met all of these testing criteria. Subsequently, a correlation analysis was performed between the monthly rainfall data from the PCH and the satellite-based GPM rainfall data. The correlation coefficient value ranges from 0 to 1, with values approaching 1 indicating a stronger or perfect correlation between the variables. Based on the correlation test results, the satellite-based GPM rainfall data compared to the PCH Kumbe data for the 2011–2024 period showed a correlation coefficient (r) of 0.77. After the calibration process, this value indicates a significant correlation between the two datasets.

Table 3. GPM Grid Coefficient Value.

Grid	Watershed Area (Km <sup>2</sup> )	Coef.
Grid 1	2.64	0.038
Grid 2	47.44	0.681
Grid 3	19.56	0.281
Total	69.64	1.00

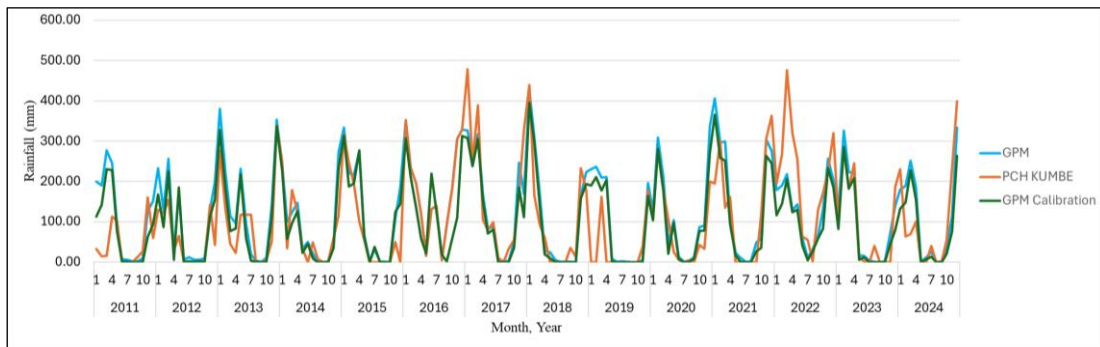


Figure 7. Correlation Test Graph between GPM Rainfall and Rainfall Observation Station (PCH).

The spatial extent of rainfall influence area derived from GPM data, along with the location of the PCH Kumbe, is shown in Figure 8.

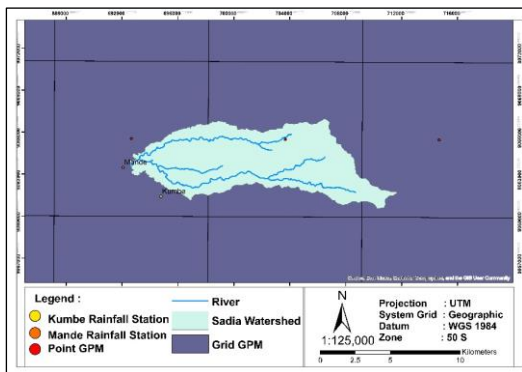


Figure 8. GPM Grid Polygon within Sadia Watershed and the Location of Kumbe (PCH).

Subsequently, the Root Mean Square Error (RMSE) was used to measure the error level in predicting annual maximum daily rainfall. The closer the RMSE value is to 0, the more accurate the prediction. The annual maximum daily rainfall (AMDR) data before correction showed an RMSE value of 0.03, while after correction using Rainfall Observation Station (PCH Kumbe) data, the RMSE value decreased to 0.01. The correction test results are presented in Figure 9.

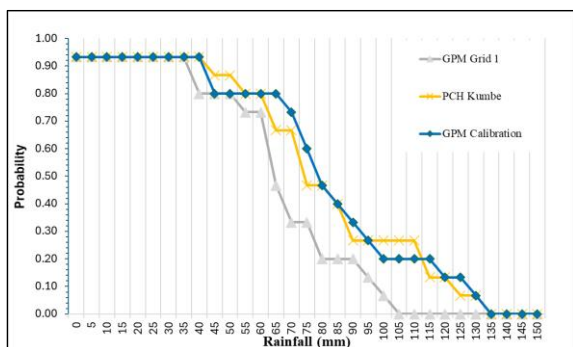


Figure 9. Corrected AMDR Probability Curve

### 3.4.2 Design Rainfall

Frequency analysis to determine the design rainfall for specific return periods can be conducted using various distribution methods, including the Normal Distribution, Log-Normal Distribution, Gumbel Distribution, and Log-Pearson Type III Distribution, as presented in Table 4. The frequency analysis was applied to the annual maximum daily rainfall (AMDR) data of the study area. Goodness-of-fit tests were performed using the Chi-square test and the Smirnov-Kolmogorov test. Based on the analysis results, the Log-Pearson Type III distribution was identified as the most suitable method that met the statistical criteria and was therefore selected for determining the design rainfall for the Sadia Watershed.

Table 4. Design Rainfall Frequency Analysis

Return Period (Years)	Design Rainfall (mm)			
	Normal	Log Normal	Log Pearson III	Gumbel
2	80.73	77.88	78.11	77.07
5	99.48	98.13	98.21	96.77
10	109.29	110.74	110.53	109.81
25	119.75	125.98	125.22	126.29
50	126.50	136.91	135.64	138.52
100	132.58	147.56	145.68	150.66
1000	149.59	181.99	177.57	190.76
<b>Kolmogorof-Smirnov Test</b>				
$D_{max}$	0.050	0.038	0.037	0.040
$D_{kritis}$	0.270	0.270	0.270	0.270
<b>Conclusion</b>	Accepted	Accepted	Accepted	Accepted
<b>Chi-SquRE Test</b>				
$\chi^2_b$	2.50	4.50	3.50	5.50
$\chi^2_c$	7.82	7.82	7.82	7.82
<b>Conclusion</b>	Accepted	Accepted	Accepted	Accepted

### 3.4.3 Curve Number (CN) and Impervious

The computation of effective rainfall and infiltration in the HEC-HMS simulation for each sub-basin (S-1 to S-11) was influenced by land use parameters, soil classification based on Hydrologic Soil Group (HSG), and the extent of impervious area. The combination of HSG and land use types determined the

Table 5. Curve Number (CN), Time Lag (T<sub>1</sub>), Initial Abstraction (I<sub>a</sub>), and Impervious Area (Imp) Values for Each Sub-Watershed in 2015, 2019, and 2022.

Sub Watershed	Area (Km <sup>2</sup> )	HSG	Yr. 2015				Yr. 2019				Yr. 2022					
			CN	T <sub>1</sub> (Min)	I <sub>a</sub>	Imp	CN	T <sub>1</sub> (Min)	I <sub>a</sub>	Imp	CN	T <sub>1</sub> (Min)	I <sub>a</sub>	Imp		
S-1	6.08	C	81.73	28.72	11.35	5.00	C	82.14	28.35	11.05	5.00	C	81.96	28.51	11.18	5.00
S-2	3.93	C	81.23	27.31	11.74	5.00	C	82.82	25.93	10.53	5.00	C	82.13	26.52	11.05	19.79
S-3	9.57	C	81.42	37.64	11.59	5.00	C,D	82.22	36.68	10.99	5.00	C	82.38	36.48	10.86	5.00
S-4	3.21	C	81.74	35.84	11.35	6.50	C,D	84.94	32.18	9.01	6.50	C	83.23	34.12	10.24	5.00
S-5	8.63	C	81.59	45.78	11.46	5.29	C	83.05	43.64	10.36	5.29	C,D	83.50	42.99	10.04	6.50
S-6	12.75	C	81.31	46.09	11.67	5.00	C	82.12	44.90	11.06	5.00	C,D	82.27	44.69	10.95	5.38
S-7	12.31	C,D	80.31	57.70	12.46	5.87	C	82.34	54.06	10.90	6.22	C,D	83.48	52.04	10.05	6.26
S-8	10.66	C	80.93	60.24	11.97	5.25	C	82.02	58.16	11.14	5.15	C	82.07	58.07	11.10	5.33
S-9	0.21	C	79.09	24.46	13.43	9.72	C,D	78.94	24.58	13.55	8.18	C	78.79	24.69	13.68	8.18
S-10	1.30	C	81.08	43.38	11.85	17.88	C	81.06	43.40	11.87	17.63	C	80.80	43.76	12.07	5.00
S-11	0.98	C,D	82.78	38.00	10.57	19.82	C	81.22	39.97	11.74	19.79	C,D	82.77	38.01	10.57	17.64
<b>Total/Avg</b>	<b>69.63</b>		<b>81.20</b>	<b>445.15</b>				<b>82.08</b>	<b>431.84</b>				<b>82.13</b>	<b>429.88</b>		

Curve Number (CN) values, which were subsequently used to estimate direct surface runoff. Changes in soil classification from Group C to C,D in several sub-basins, including S-3, S-4, S-5, S-6, and S-7, indicated a reduction in soil infiltration capacity due to land degradation or compaction processes. This condition led to an increase in CN values and, consequently, higher effective rainfall volumes. In addition, a substantial increase in impervious area was observed in sub-basins S-2 and S-11 from 2015 to 2022, contributing to greater runoff volume and a faster watershed response time. The highest CN value in 2022 was recorded in sub-basin S-7 (CN: 83.50), indicating that this area has the highest potential for surface runoff generation, primarily due to changes in HSG classification and the expansion of dryland forest cover.

Based on the land use cover analysis, the Curve Number (CN) values and impervious area percentages influence the time of concentration and time lag, which were calculated using Equations (4) and (5) (USDA NRCS 2021).

$$T_1 = 0.6 T_c \tag{4}$$

$$T_c = \frac{L^{0.8}(S+2.54)^{0.7}}{1410Y^{0.5}} \tag{5}$$

where T<sub>1</sub> is the time lag, T<sub>c</sub> is the time of concentration, L is the flow length (m), S is the maximum potential retention, and Y is the average watershed slope.

The analysis results indicate changes in sub-watershed characteristics between 2015, 2019, and 2022. The average CN value increased from 81.20 (2015) to 82.08 (2019) and 82.13 (2022), reflecting a reduction in soil infiltration capacity.

The CN increase between 2019 and 2022 was relatively small due to the addition of plantation forests. The Time Lag (T<sub>1</sub>) decreased from 445.15 minutes (2015) to 431.84 minutes (2019) and 429.88 minutes (2022), indicating faster runoff responses as a result of expanding impervious areas. The Initial Abstraction (I<sub>a</sub>) values remained relatively stable, while the impervious area percentages (Imp) in several sub-watersheds, such as S-2 and S-11, increased significantly, accelerating surface runoff and raising flood potential. The calculated values of CN, T<sub>1</sub>, I<sub>a</sub>, and Imp for each sub-watershed in 2015, 2019, and 2022 are presented in Table 5

### 3.5 Design Flood Discharge

Design flood discharge analysis for a 25-year return period (Q<sub>25</sub>) was conducted using the Synthetic Unit Hydrograph (SUH) method of SCS-CN through the HEC-HMS model. The design flood discharge analysis for a 25-year return period (Q<sub>25</sub>) was conducted using the Synthetic Unit Hydrograph (SUH) method from the SCS-CN approach through HEC-HMS modeling. The input parameters included loss parameters (initial abstraction, curve number (CN), and impervious area), transformation (time lag), and routing (Muskingum), with values presented in Table 5. The hydrological input comprised the hourly distribution of rainfall for various return periods, which had been analyzed in the previous stage. To determine the design discharge, the 2-year return period discharge (Q<sub>2</sub>) was compared to the bankfull discharge measured in an unaffected section of the Sadia River. The measurement location was Sadia River STA 3063.95/P.22 in the upstream section, as shown in Figure 11. The bankfull discharge was estimated using a trial-and-error approach with the HEC-RAS 1D model under unsteady flow conditions. The upstream boundary condition (BC) at point J1 was entered into the model to simulate the river's response to flood

discharge. This resulted in a bankfull discharge value of 95.65 m<sup>3</sup>/s.

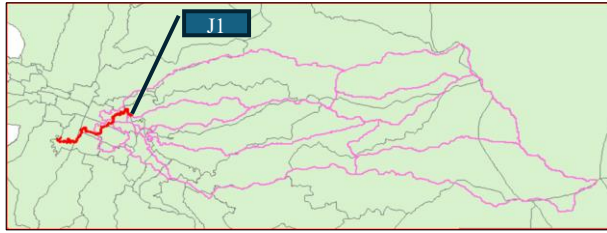
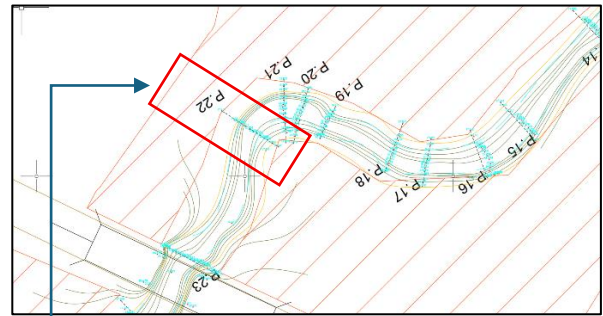


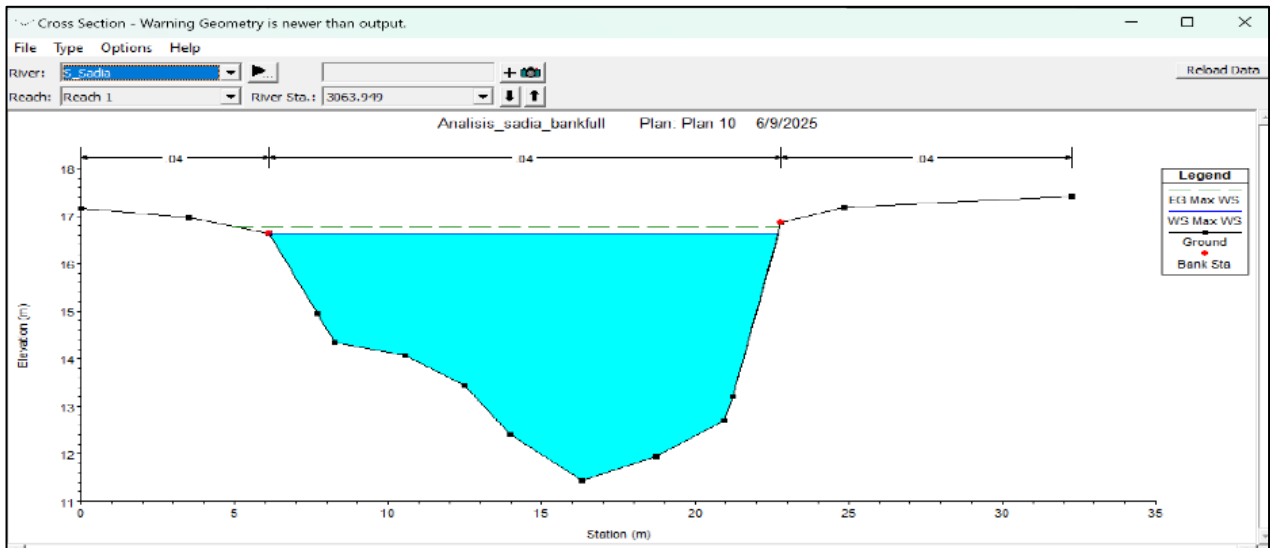
Figure 10. Inlet Point of the Sadia River (J1).



(b)



(a)



(c)

Figure 11. (a) Sadia River, (b) Bankfull Discharge Location at Sadia River (c) Typical Bankfull Discharge.

Profile Output Table - Standard Table 1												
HEC-RAS Plan: Plan 10 River: S_Sadia Reach: Reach 1 Profile: Max WS												
Reach	River Sta	Profile	Q Total (m <sup>3</sup> /s)	Min Ch El (m)	W.S. Elev (m)	Crit W.S. (m)	E.G. Elev (m)	E.G. Slope (m/m)	Vel Chnl (m/s)	Flow Area (m <sup>2</sup> )	Top Width (m)	Froude # Chl
Reach 1	3092.104	Max WS	95.69	12.46	16.66		16.82	0.001484	1.79	53.60	18.08	0.33
Reach 1	3083.838	Max WS	95.68	12.38	16.64		16.81	0.001585	1.81	52.83	18.69	0.34
Reach 1	3063.949	Max WS	95.65	11.44	16.63		16.78	0.001327	1.74	55.08	16.58	0.30
Reach 1	2992.701	Max WS	95.56	12.81	16.54		16.68	0.001454	1.68	56.80	21.57	0.33

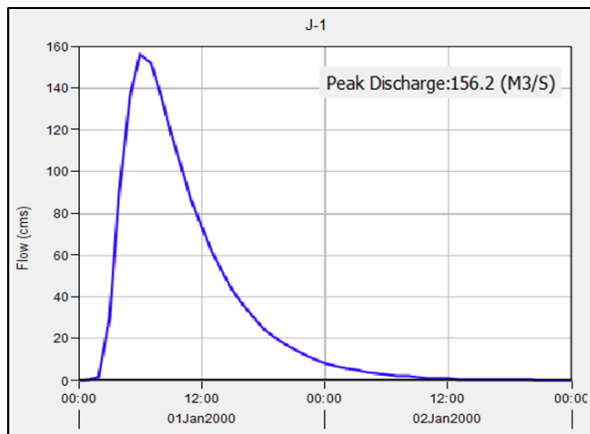
Total flow in cross section.

Figure 12. Bankfull Discharge Modeling Result of the Sadia River.

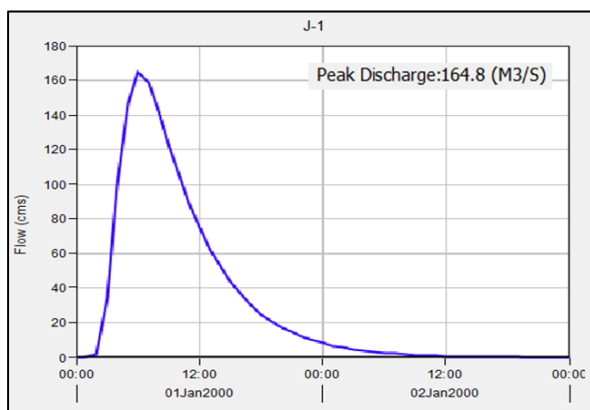
Based on the analysis of the design flood discharge for the 2022 land use condition, the SCS-CN method produced a peak flood discharge ( $Q_2$ ) of 79,20  $m^3/s$ . This value closely approximates the observed  $Q_2$  flood discharge of the Sadia River, indicating that the SCS-CN method can be reliably applied for estimating the  $Q_{25}$  design flood discharge. The results of the design flood discharge analysis with a 25-year return period ( $Q_{25}$ ) using the Synthetic Unit Hydrograph (SUH) SCS method for the 2015, 2019, and 2022 land use conditions are presented in Table 6.

Table 6. Design Flood Discharge Using the SCS-CN Method  $Q_{25}$

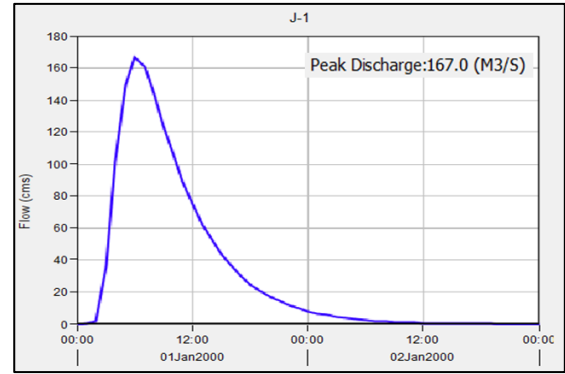
Land Use Cover Year	Peak Discharge ( $m^3/s$ )	Avg. CN	Time lag ( $T_l$ ) (min)
2015	156,20	81.20	445,15
2019	164,80	82.08	431,84
2022	167,00	82.13	429,88



(a)



(b)



(c)

Figure 13.  $Q_{25}$  Flood Hydrograph from HEC-HMS Model for Land Use Cover (a) 2015, (b) 2019, and (c) 2022.

### 3.6 The Relationship Between Land Use Change and Its Impact on Time Lag and Peak Flood Discharge

The SCS-CN method is capable of integrating land use, soil type, and initial moisture condition parameters to spatially estimate surface runoff (Kumar et al. 2021) and it demonstrates high accuracy in representing design discharge in response to land cover changes (Wahyuni and Sachro 2024). The HEC-HMS simulation using the SCS-CN method ( $Q_{25}$ ) indicates that land cover changes in 2015, 2019, and 2022 have led to an increase in peak discharge and a reduction in time lag of runoff entering the Sadia River. As shown in Table 6, peak discharge increased from 156,20  $m^3/s$  (2015) to 164,80  $m^3/s$  (2019), and further to 167,00  $m^3/s$  (2022), corresponding to an increase in Curve Number (CN) values from 81.20 to 82.08 and 82.13, respectively. Concurrently, the time lag decreased from 445.15 minutes (2015) to 431.84 minutes (2019), and 429.88 minutes (2022), indicating a more rapid runoff response. The flood hydrographs generated from the HEC-HMS model show that the 2015 hydrograph exhibited a flatter and delayed peak compared to 2019 and 2022. In contrast, the 2022 hydrograph presented a steeper curve with a higher peak discharge, suggesting increased surface runoff velocity and volume as a result of land cover change.

Therefore, the land use change that occurred between 2015 and 2022 has been shown to increase peak discharge and reduce time lag, ultimately heightening the flood risk in the vicinity of the Sadia River. It is important to note that land cover changes not only affect hydrological characteristics, but also increase the potential for faster and more intense flash flooding. In this context, land use planning and management play a critical role in reducing the impacts of flood disasters. The development of sustainability-based mitigation strategies that incorporate ecological and socio-economic considerations, such as reforestation and improvements to urban drainage

systems, is essential to address the growing risks posed by ongoing land conversion and climate change.

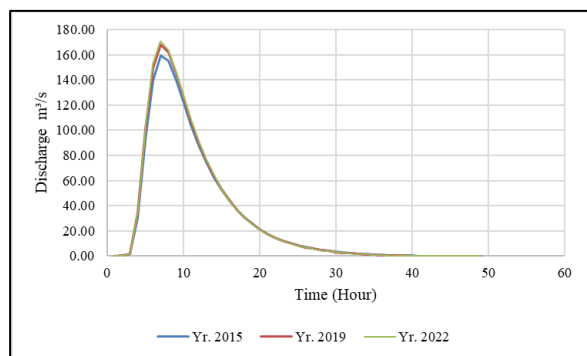


Figure 14. Sadia River Flood Hydrograph  $Q_{25}$  SCS-CN Methods.

#### 4. Conclusion

The findings of this study demonstrate that changes in land use within the Sadia Watershed, particularly the substantial growth of dryland agricultural areas from 12.67% in 2015 to 37.41% in 2022, have significantly impacted the watershed's hydrological response. This expansion occurred at the expense of vegetative land covers, such as secondary forests and shrublands. Consequently, there was an increase in impervious surface areas and a reduction in soil infiltration capacity, especially in sub-watersheds S-2 and S-11. Consequently, peak discharge under the 25-year return period ( $Q_{25}$ ) increased from 159.50 to 170.50  $m^3/s$ , while the time lag decreased from 445.15 to 429.88 minutes, indicating a faster runoff response. These hydrological shifts are supported by an increase in the Curve Number (from 81.20 to 82.13), which reflects a decline in infiltration potential. While intensified rainfall contributes to these outcomes, land use changes are identified as the predominant factor. Therefore, integrated watershed management is required to mitigate future flood risks, including the implementation of revegetation strategies, land conversion restrictions, drainage system improvements, and climate-responsive planning.

#### Acknowledgment

The authors would like to express their sincere appreciation to the Master Program in Water Resources Management, Institute Technology of Bandung, the Human Resources Development Agency (BPSDM) of the Ministry of Public Works, and River Basin Organization for Nusa Tenggara I (BBWS Nusa Tenggara I) in Mataram, Ministry of Public Works, for their support in the preparation and publication of this manuscript.

#### References

- Balai Teknik Bendungan. 2022. *Modul 1-Analisis Curah Hujan*.
- Farid, Mohammad, Bachroni Gunawan, Muhammad Syahril Badri Kusuma, Suyudi Akbari Habibi, and Alkindi Yahya. 2020. "Assessment of Flood Risk Reduction in Bengawan Solo River: A Case Study of Sragen Regency." *International Journal of GEOMATE* 18(70): 229–34. doi:10.21660/2020.70.18010.
- Formánek, Adam, Rasmiaditya Silasari, M. Syahril Badri Kusuma, and Hadi Kardhana. 2013. "Two-Dimensional Model of Ciliwung River Flood in DKI Jakarta for Development of the Regional Flood Index Map." *Journal of Engineering and Technological Sciences* 45 B(3): 307–25. doi:10.5614/j.eng.technol.sci.2013.45.3.7.
- Gunawan, Taufik Ari, M Syahril, Badri Kusuma, M Cahyono, and Joko Nugroho. 2016. "The Application of Backpropagation Neural Network Method to Estimate the Sediment Loads." In *MATEC Web Conferences 101, 05016 (2017)*, EDP Sciences, 101. doi:10.1051/mateconf/201710105016.
- Handyastono, B., M. A. Alghoul, A. Rizki, N. P. Djambek, M. S.B. Kusuma, A. A. Kuntoro, D. Harlan, et al. 2025. "Flood Hazard Assessment in Pemaluan Village Due to Land Use Change in IKN (Ibu Kota Nusantara) as the New Capital City of Indonesia." *Case Studies in Chemical and Environmental Engineering* 11(March): 101211. doi:10.1016/j.cscee.2025.101211.
- Hartyan, Suripin. 2024. "Pemodelan Debit Banjir Rencana Berbasis Data Hujan Satelit Pada Daerah Tangkapan Air Bendungan Meninting." 30(1): 1–8. doi:10.14710/mkts.v30i1.59024.
- Juliana, Imroatul C., M. Syahril Badri Kusuma, M. Cahyono, Widjaja Martokusumo, and Arno Adi Kuntoro. 2017. "The Effect of Differences Rainfall Data Duration and Time Period in the Assessment of Rainwater Harvesting System Performance for Domestic Water Use." In *AIP Conference Proceedings*, American Institute of Physics Inc. doi:10.1063/1.5011616.
- Kardhana, Hadi, Jonathan Raditya Valerian, Faizal Immaddudin Wira Rohmat, and Muhammad Syahril Badri Kusuma. 2022. "Improving Jakarta's Katulampa Barrage Extreme Water Level Prediction Using Satellite-Based Long Short-Term Memory (LSTM) Neural Networks." *Water (Switzerland)* 14(9). doi:10.3390/w14091469.
- Kumar, Abanish, Shruti Kanga, Ajay Kumar Taloor, Suraj Kumar Singh, and Bojan Đurin. 2021. "Surface Runoff Estimation of Sind River Basin Using Integrated SCS-CN and GIS Techniques." *HydroResearch* 4: 61–74. doi:10.1016/j.hydres.2021.08.001.

- Kuntoro, Arno Adi, Anton Winarto Putro, M. Syahril B. Kusuma, and Suardi Natasaputra. 2017a. "The Effect of Land Use Change to Maximum and Minimum Discharge in Cikapundung River Basin." In *AIP Conference Proceedings*, American Institute of Physics Inc. doi:10.1063/1.5011621.
- Kuntoro, Arno Adi, Anton Winarto Putro, M. Syahril B. Kusuma, and Suardi Natasaputra. 2017b. "The Effect of Land Use Change to Maximum and Minimum Discharge in Cikapundung River Basin." *AIP Conference Proceedings* 1903(July). doi:10.1063/1.5011621.
- Merwade, Venkatesh. 2022. "Hydrologic Modeling Using HEC-HMS Opening / Creating a HEC-HMS Project." : 1–27.
- Mufrodi, Syahrizal, and Ignatius Sriyana. 2024. "Analisis Pengaruh Perubahan Karakteristik DAS Terhadap Keamanan Bendungan Pamukkulu Berdasarkan Penelusuran Banjir." *Teknik* 45(1): 1–10. doi:10.14710/teknik.v45i1.59399.
- PUPR, Kementerian. 2021. "PERMEN PUPR Republik Indonesia Nomor 5 Tahun 2021." *Petunjuk Operasional Pengelolaan Dana Alokasi Khusus Infrastruktur Pekerjaan Umum Dan Perumahan Rakyat Tahun Anggaran 2021* (3): 95–140.
- Rizaldi, Akbar, Muhammad Syahril Badri Kusuma, Arno Adi Kuntoro, and Hadi Kardhana. 2022. "Trend Analysis of Rainfall, Land Cover, and Flow Discharge in the Citarum Hulu–Majalaya Basin." *International Journal on Advanced Science, Engineering and Information Technology* 12(4): 1469–77. doi:10.18517/ijaseit.12.4.15225.
- Rizaldi, Akbar, Muhammad Syahril, Badri Kusuma, Arno Adi Kuntoro, and Hadi Kardhana. 2022. "Trend Analysis of Rainfall, Land Cover, and Flow Discharge in the Citarum Hulu–Majalaya Basin." 12(4).
- Sachro, Sri Sangkawati, Sutarto Edhisono, Pranoto Samto Atmodjo, and Wahyu Prasetyo. 2017. "Korelasi Klasifikasi Penutup Lahan Dengan Debit Puncak Di Daerah Aliran Sungai." *Media Komunikasi Teknik Sipil* 23(2): 157. doi:10.14710/mkts.v23i2.16687.
- Sultan, Dagnenet, Atsushi Tsunekawa, Mitsuru Tsubo, Nigussie Haregeweyn, Enyew Adgo, Derege Tsegaye Meshesha, Ayele Almaw Fenta, et al. 2022. "Evaluation of Lag Time and Time of Concentration Estimation Methods in Small Tropical Watersheds in Ethiopia." *Journal of Hydrology: Regional Studies* 40(September 2021): 101025. doi:10.1016/j.ejrh.2022.101025.
- Taufik, S. R., M. Yatrib, A. N. Harman, T. N.A. Kesuma, D. Saputra, and M. S.B. Kusuma. 2022. "Assasment of Flood Hazard Reduction in DKI Jakarta: Bendungan Hilir Village." *IOP Conference Series: Earth and Environmental Science* 989(1). doi:10.1088/1755-1315/989/1/012018.
- Triatmodjo, Bambang. 2019. *Hidrologi Terapan (7 Ed.)*. Beta Offset, Yogyakarta.
- USDA NRCS. 2021. "Engineering Field Handbook Chapter 2: Estimating Runoff and Peak Discharges." *National Engineering Handbook*.
- Wahyuni, Indah Tri, and Sri Sangkawati Sachro. 2024. "The Impact of Land Cover Changes on Flood Hydrograph Characteristics (Jragung Dam Case Study)." *Media Komunikasi Teknik Sipil* 29(2): 280–88. doi:10.14710/mkts.v29i2.59877.
- Yasa, I Wayan, Salehudin, Humairo Saidah, I Dewa Gede Jayanegara, and Heri Sulistiyono. 2023. "Analisis Pola Sebaran Karakteristik Iklim Di Pulau Sumbawa." *Ganec Swara* 17(4): 1373. doi:10.35327/gara.v17i4.619.
- Yosua, Horas, Muhammad Syahril Badri Kusuma, and Joko Nugroho. 2023. "An Assessment of Pluvial Hazard in South Jakarta Based on Land-Use/Cover Change from 2016 to 2022." *Frontiers in Built Environment* 9(January): 1–8. doi:10.3389/fbuil.2023.1345894.